Menger-Slice Inspired Fractals based on the Pentagon, Dodecahedron, and 120-Cell

Rob Hocking

Taipei City, Taiwan; rob.l.hocking@gmail.com

Abstract

When the 3D Menger sponge is sliced with a suitably chosen diagonal plane, a novel 2D fractal consisting of a hexagon with fractal hexagram stars emerges. In this work I attempt to create an analogous fractal using pentagons and pentagrams. Unlike in the case of Menger-slice, the mathematics is less perfect with no clear best answer. I propose three solutions, each with their own pros and cons, but acknowledge the possibility of other, better solutions that I have not thought of. I then generalize these ideas to the dodecahedron in 3D as well as the 120-cell in 4D and 3D print the fractals that result.

Introduction

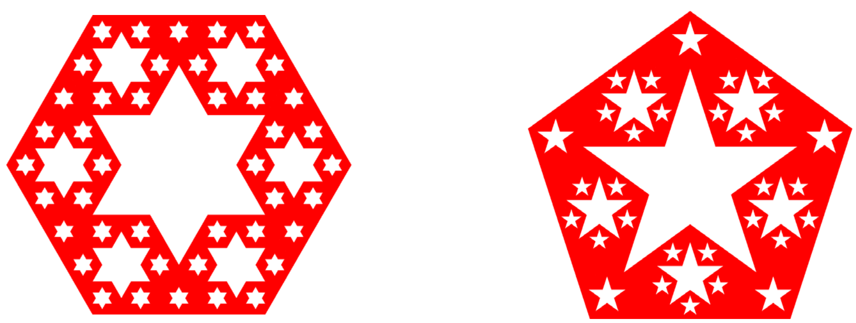

(a) **(b)**

Figure 1: *The Menger-slice fractal discovered in 2007 by Sébastien Pérez-Duarte (a), and one of three attempted generalizations using pentagons and pentagrams by the author (b).*

The Menger sponge is a well known fractal first described in 1926 by Karl Menger [5], which was shown in 2007 by Sébastien Pérez-Duarte to produce the 2D fractal illustrated in Figure 1(a) when chopped with an appropriate diagonal plane [2]. When I first saw the Menger-slice fractal in 2022, two questions immediately flashed through my mind. First, I wondered what would happen if one instead took 3D cross-sections of 4D Menger sponges; this was the subject of my previous work [3]. Second, I wondered if something like this could be made to work for pentagons and pentagrams rather than hexagons and hexagrams; something like Figure 1(b). The fact that the latter exists suggests that the answer is "yes", but a better answer might be "kind of". Getting something like the Menger-slice to work for pentagons involves cheating and trade-offs, with no obvious best answer. Exploring this is, in part, the purpose of the present work (and indeed, we will consider three possible solutions). I say "in part" because the pentagon can be generalized in 3D to the dodecahedron and in 4D to the 120-cell. This is why I picked it rather than some other n-gon. After exploring the 2D case, we will generalize our approach to 3D and to 4D, creating along the way fractals that we can 3D print.

Before we dive into things, the first thing we need to do is forget that the Menger-slice is a cross-section of something. Searching for a generalization by chopping open ever more exotic 3D fractals and hoping for a miracle did not work out very well for me in the early stages of this project. Instead we will view it as a *closed fractal family*, which I now define.

Definition 1. *A family of fractals $\mathcal{F}$ is a* closed fractal family *if each member of $\mathcal{F}$ can be expressed as a union of scaled, translated, and possibly rotated and/or reflected copies of itself and other members of the family.*

The literature uses the term "directed-graph iterated function system" rather than "closed fractal family" [4] but I find that name opaque and un-intuitive, so I will not be using it in this paper. Finally, let's give our generalization a name: the "Pentagon-pentagram fractal".

The Menger-Slice as a Closed Fractal Family

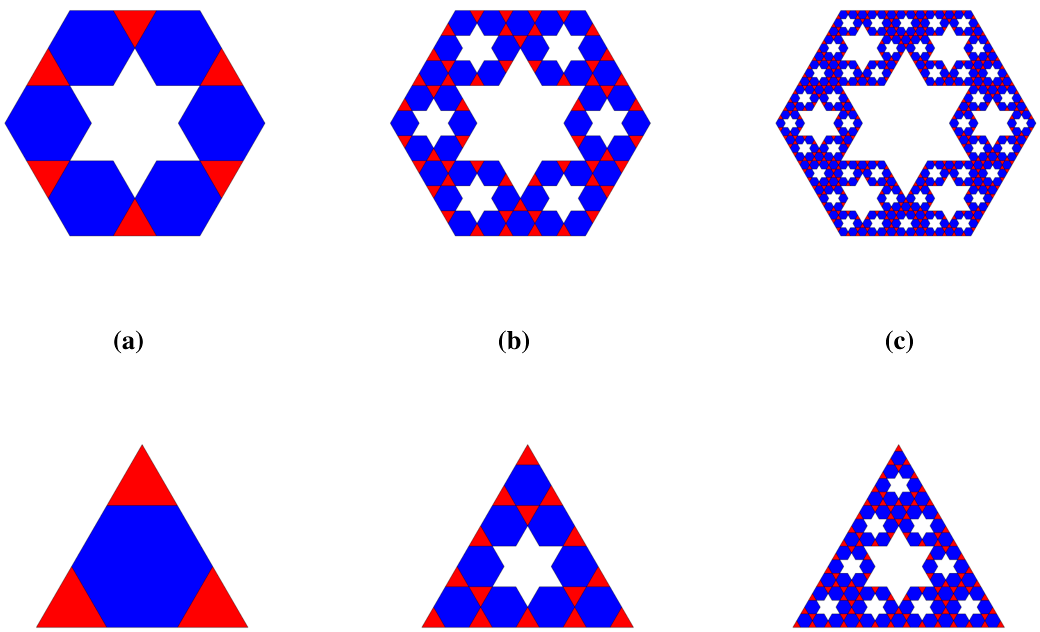

(a) **(b)** **(c)**

(d) **(e)** **(f)**

Figure 2: *The Menger-slice as a closed fractal family. In (a)–(c) we see the first three iterations of the Menger-slice, while (d)–(f) show the first three iterations of the triangle fractal it is coupled to.*

It is possible to view the Menger-slice as a purely 2D fractal, without knowing anything about Menger sponges or even the existence of a third dimension. The starting point for this is the two pictures in Figure 2(a) and Figure 2(d). The key observation is that a hexagon can be constructed out of smaller hexagons and triangles, while the same is true of a triangle. Leaving out from the hexagon the centermost of the smaller hexagons and the triangles surrounding it leaves a hexagram shaped hole; this is a Menger-slice with recursion depth one. Next, we replace each of the hexagons in Figure 2(a) and Figure 2(d) with a scaled down copy of 2(a), and each of the triangles with a scaled down copy of 2(d). This yields the recursion depth two hexagon and triangle fractals shown in Figure 2(b) and 2(e). The recursion depth three fractals are obtained by replacing each of the hexagons in Figure 2(a) and 2(d) with a scaled down copy of 2(b), and each of the triangles with

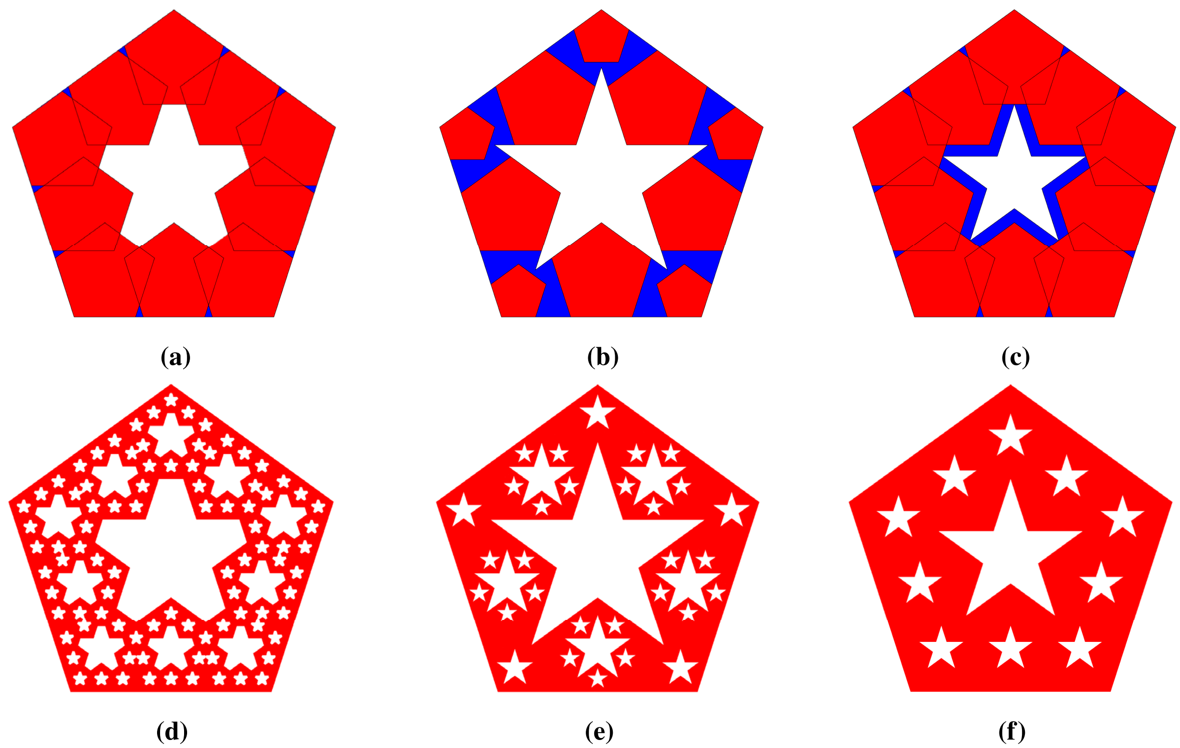

Figure 3: *Three versions of the Pentagon-pentagram fractal. In (a)–(c), we show three possible setups, with sub-pentagons in red and filler pieces in blue. In (d)–(e), we see the result of substituting shrunk down copies of (a)–(c) into the smaller sub-pentagons, with tie-breaker logic to handle overlap.*

a scaled down copy of 2(e). The results are illustrated in Figure 2(c) and 2(f). This a closed fractal family with two members, the Menger-slice hexagon fractal H and a triangle fractal T (which, it turns out, can also be expressed as a slice of the Menger sponge). Denoting by $H^{(n)}$ and $T^{(n)}$ the nth iteration of our fractal hexagon and triangle respectively, the above fractal recursion can be described in terms of equations as:

$$
\begin{aligned}
H^{(n+1)} &= \bigcup_{i=1}^{6}\left(\frac{H^{(n)}}{s}+\vec{t}^{\,i}_{H,H}\right)+\bigcup_{i=1}^{6}\left(\frac{T^{(n)}}{s}+\vec{t}^{\,i}_{H,T}\right)\\
T^{(n+1)} &= \frac{H^{(n)}}{s}+\bigcup_{i=1}^{3}\left(\frac{T^{(n)}}{s}+\vec{t}^{\,i}_{T,T}\right).
\end{aligned}
$$

Here, we have scale factor $s = 3$, the translation vectors $\vec{t}^{\,i}_{H,H}$ and $\vec{t}^{\,i}_{H,T}$ can be expressed in terms of the sixth roots of unity, and the translation vectors $\vec{t}^{\,i}_{T,T}$ can be expressed in terms of the third roots of unity.

The Pentagon-Pentagram Fractal as a Closed Fractal Family

The starting point for the Pentagon-pentagram fractal is Figure 3(a), which expresses a larger pentagon in terms of ten smaller sub-pentagons (red), a large pentagram-shaped hole (white), and some filler pieces (blue). We can see immediately that the geometry is not as perfect as it was in the previous section. The sub-pentagons overlap. The tips of the pentagram are chopped off. The filler pieces cannot be expressed in terms of smaller copies of themselves and sub-pentagons, and therefore will not fill up with new details as we iterate. However, my goal is to make fractals that can be 3D printed, and we hit the resolution limit of most 3D printers after about three iterations. The hope is that for such a small number of iterations, the filler pieces will not be too conspicuous.

Figure 3(c) shows the result of plugging a scaled down version of Figure 3(a) into each of the ten sub-pentagons contained there, to a recursion depth of three, with the addition of some tie-breaking logic to handle overlap. Specifically, if a point belongs to two sub-pentagons simultaneously, we say that it is part of a hole if it is so in *either* sub-pentagon. In formulas, we have:

$$P^{(n+1)} = \bigcup_{\vec{t}\in T} \left\{ \frac{P^{(n)}}{s} + \left(1 - \frac{1}{s}\right)\vec{t} \right\} + \text{filler pieces} + \text{tie-breaker logic.} \tag{1}$$

where $T = V \cup E$, with V denoting the vertices of the original pentagon $P^{(0)}$, and E the midpoints of its edges. The scale factor is chosen as $s = 3.25$ in this case, as this results in perfect overlap of the smallest stars closest to the main central star in overlapping regions, making the tie-breaker logic redundant. However, one can see that the second layer of the smallest stars a bit further out overlap each other and merge; this is due to the choice of tie-breaker logic used, as described above.

This is nice, but one is left wondering if there is some way to get full pentagram stars rather than "chopped" pentagrams. The first strategy is to extend to a point the tips of the central star in Figure 3(a) into five of the ten sub-pentagons, which shrink down in size to get out of the way. The result is shown in 3(b). However, these smaller pentagons are not used until the third recursion step, meaning that this fractal uses different recursion rules at different steps. In this case, $P^{(1)}$ and $P^{(2)}$ are constructed using (1) with $T = E$, while for $P^{(3)}$ we use the modified formula:

$$P^{(3)} = \bigcup_{\vec{t}\in E} \left\{ \frac{P^{(2)}}{s} + \left(1 - \frac{1}{s}\right)\vec{t} \right\} + \bigcup_{\vec{t}\in V} \left\{ \frac{P^{(1)}}{\alpha s} + \left(1 - \frac{1}{\alpha s}\right)\vec{t} \right\} + \text{filler pieces.} \tag{2}$$

In Figure 3(b) I have chosen $s = 3.25$ and $\alpha = 1.8$, and the third iteration $P^{(3)}$ is shown in Figure 3(e). An advantage of this setup is that there is no overlap of the sub-pentagons and hence no tie-breaker logic is required.

The second strategy, illustrated in Figure 3(c), is to add additional filler pieces that narrow the pentagram down until it is no longer chopped off. This strategy works well for two iteration steps, as shown in Figure 3(f) with $s = 3.25$. However, by the third step these extra filler pieces become conspicuous, and so we limit ourselves to two steps in this case. Despite this limitation, this strategy is especially effective in three dimensions, which we turn to now.

The Dodecahedron-Pentagram Fractal

Having tackled the 2D case of a pentagon, we now move on to the 3D case of a dodecahedron in the hopes that some of the insights we have gained will carry over. We are in luck; the exact same strategies we employed in 2D carry over essentially without change to 3D. Equations (1) and (2) may be used without modification, so long as we now interpret $P^{(0)}$ as a dodecahedron, V the set of its twenty vertices, and E the set of midpoints of its thirty edges. We also change the tie-breaker logic so that if a point belongs to two sub-dodecahedrons simultaneously, it has to be part of a hole in *both* of them to be considered part of a hole in the overall fractal. Otherwise, we end up with fractals that are "too holey" and difficult to 3D print. The straightforward 3D generalizations of Figure 3(a)–(c) are illustrated in Figure 4(a)–(c), where sub-dodecahedrons are colored red, and filler pieces are colored blue.

Aside from the difference in tie-breaker logic, the main difference with the 2D case is that in 3D the holes in the fractal narrow as you move towards the center, due to the "roundness" of the sub-dodecahedrons. This can be seen clearly in Figure 4(a)–(b). It means that we need larger values of s than we did in 2D if we want to be able to see inside the fractal. Just like in 2D, there are three cases to consider:

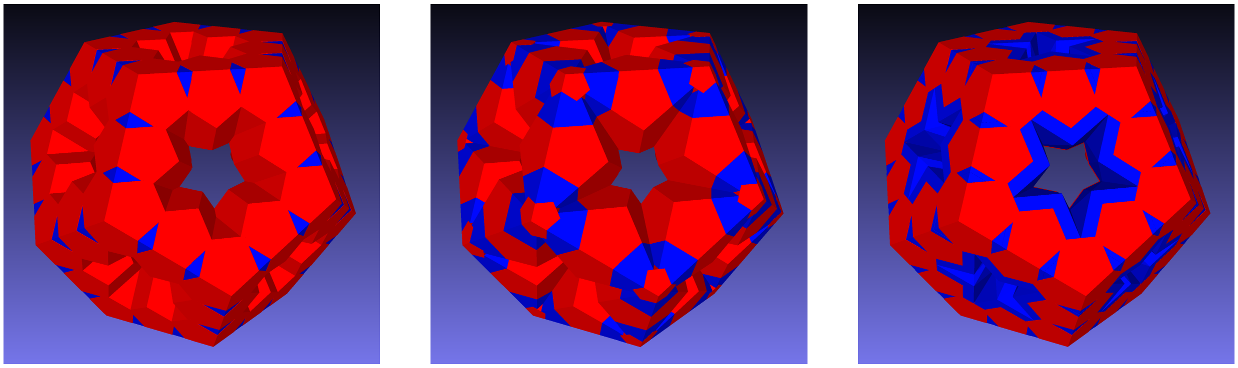

(a) **(b)** **(c)**

Figure 4: *Generalizations to 3D of the setups in Figure 3(a)–(c). Sub-dodecahedrons are colored red, while filler pieces are colored blue.*

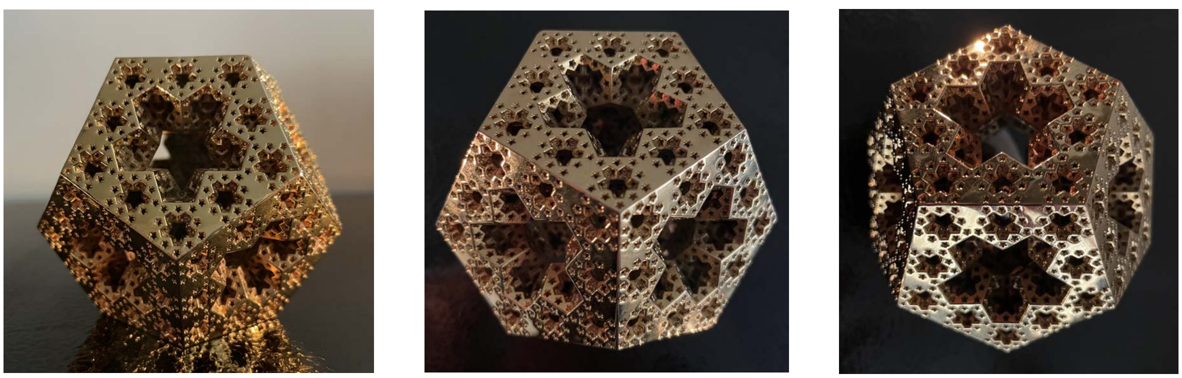

(a) **(b)** **(c)**

Figure 5: *Three recursion steps of the setup in Figure 4(a).*

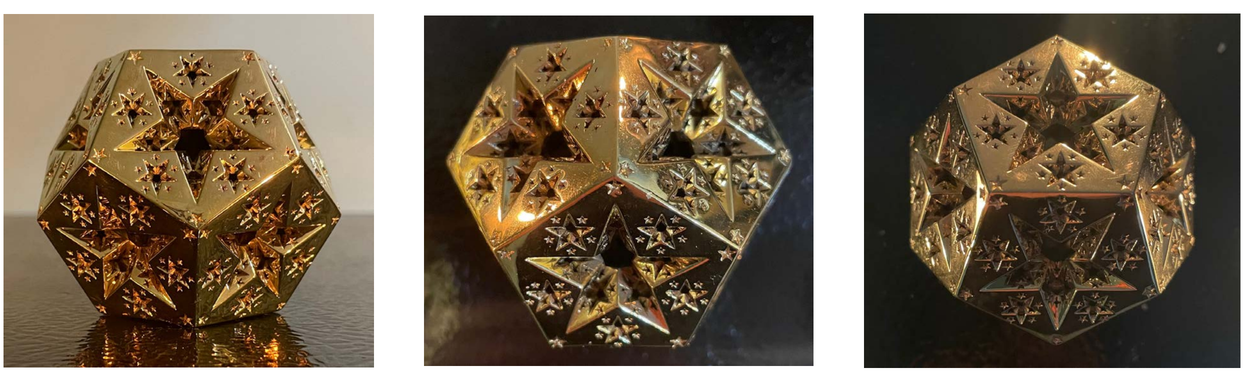

(a) **(b)** **(c)**

Figure 6: *Three recursion steps of the setup in Figure 4(b).*

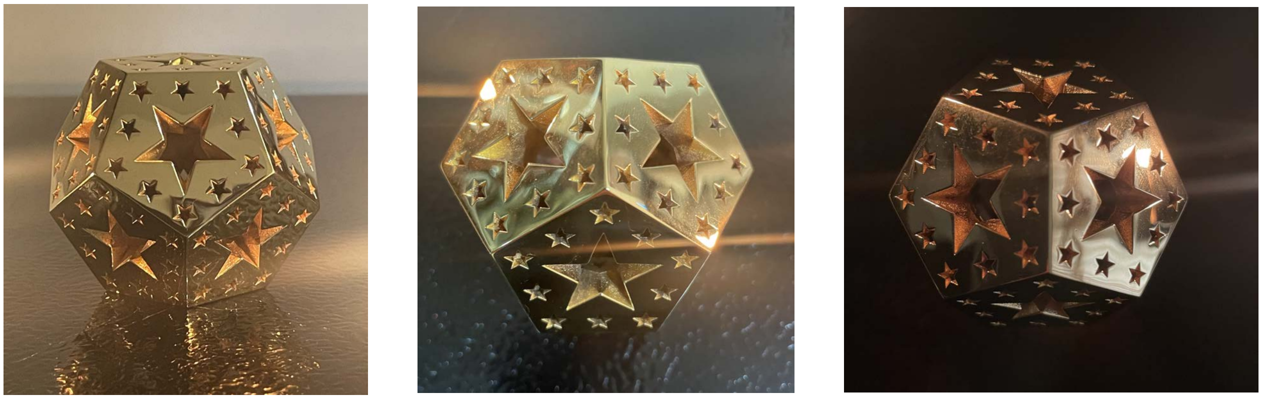

(a) **(b)** **(c)**

Figure 7: *Two recursion steps of the setup in Figure 4(c).*

1. Leaving the chopped pentagrams alone, as in Figure 4(a).
2. Correcting the chopped pentagrams by extending them, as in Figure 4(b).
3. Correcting the chopped pentagrams by narrowing them with additional filler pieces, as in Figure 4(c).

The first strategy results in the 3D printed fractal shown in Figure 5, and uses $s = 4$. This large value of s is needed due to the narrowing effect described above. Note the presence of intricate star-patterns on the walls of each star shaped hole as it tapers inwards. For the second strategy, we use $s = 3.5$ and $\alpha = 2.41$. The logic is again virtually unchanged from the 2D case, see Figure 6. The third strategy is especially powerful in three dimensions, because the filler pieces can be designed to reduce the "roundness" of the sub-dodecahedrons, so that the tapering effect discussed above is largely eliminated, see Figure 4(c). Figure 7 shows the result of this approach as a 3D printed fractal with $s = 3.9$.

The 120-Cell Fractal

Just as twelve pentagons may be joined together in 3D to form a dodecahedron, so 120 dodecahedrons may be joined together in 4D to the a closed hypersurface called the 120-cell. Readers unfamiliar with the 120-cell may find [7], for example, to be a good place to start.

To extend the ideas above into the fourth dimension, I have taken a simple approach. Rather than create a true fractal 120-cell (perhaps a project for another day), I have simply taken a hollow 120-cell and replaced each of the dodecahedrons making up its surface with one of the fractal dodecahedrons from the previous section. For simplicity, I always use the fractal from Figure 5 with a recursion depth of two. I then project the result down to 3D, in the form of a Schlegel diagram [1].

Rather than print the full 120-cell, I print a few judiciously picked subsets. For this, it is helpful to know something about the geometric (or algebraic) structure of the 120-cell; specifically that it may be partitioned into twelve disjoint rings of ten dodecahedrons each. This is something that is well known and I will not delve into the details other than to say that I found Segerman and Schleimer's paper [6] to be a helpful resource.

One of the "rings" is a perfectly vertical central ring, and it has five rings wrapping around it, all of which are identical up to a rigid motion of $\mathbb{R}^3$. Figure 8(a) shows three such identical rings—3D printed in different metals—side by side, while Figure 8(b) shows how they fit together. Keeping all five rings but printing in nickel-plated plastic yields a tree-like structure with a central vertical hole as in 8(c). If a rod shaped light source is placed in the central cavity and the lights are turned off, an interesting pattern of shadows and pentagram-shaped spots of light is created as in Figure 8(d). Another interesting set of rings

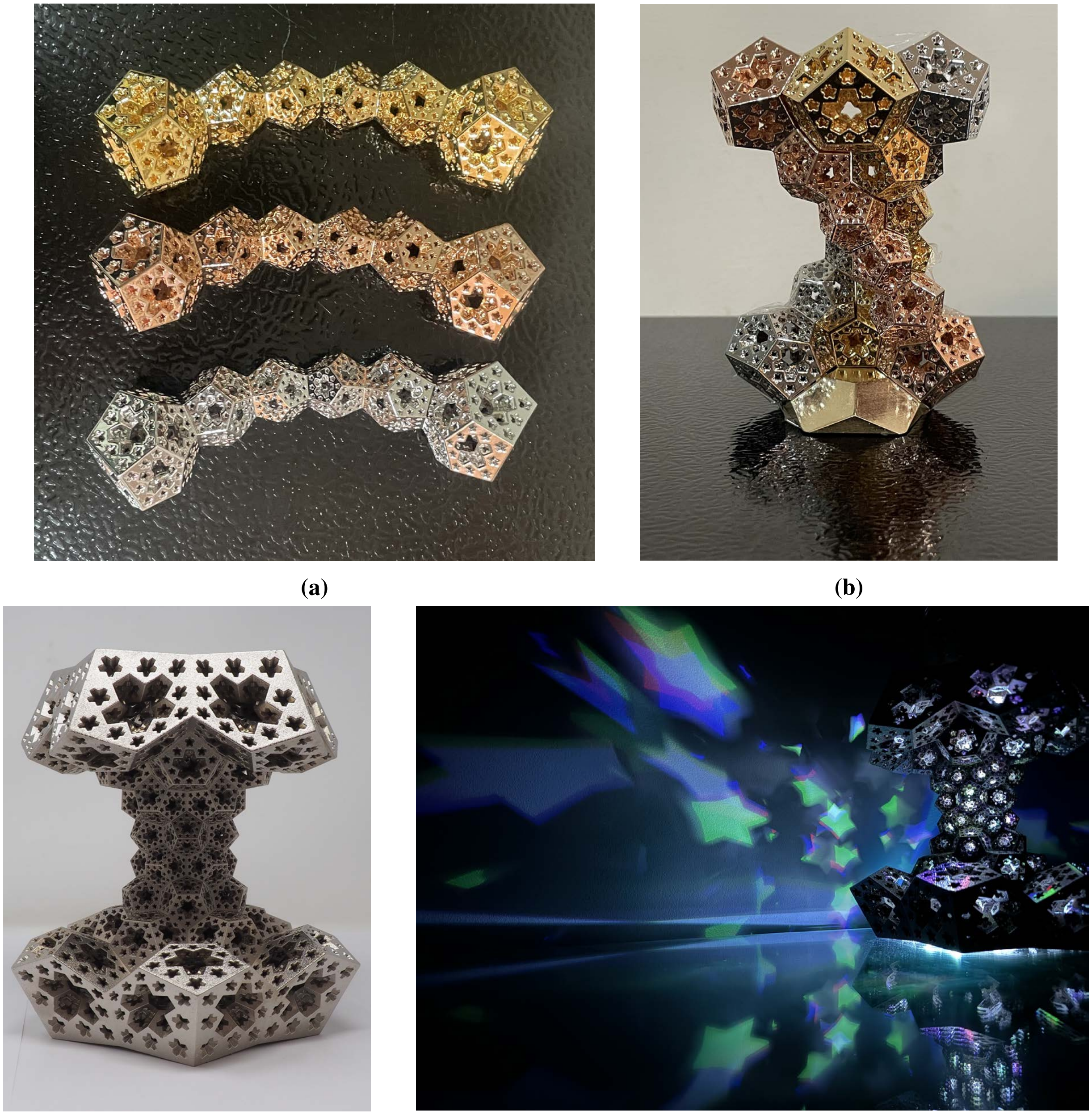

(a) **(b)**

(c) **(d)**

Figure 8: *In (a) we see 3D prints of three of the five identical—up to a rigid motion of $\mathbb{R}^3$—rings of fractal dodecahedrons surrounding the vertical central ring in the 120-cell fractal. In (b), these three rings have been fit together so that they wrap around the missing central ring. In (c), we now have all five of the rings twisting around the central cavity. In (d), we have placed a vertical light source within the central cavity and turned off the lights.*

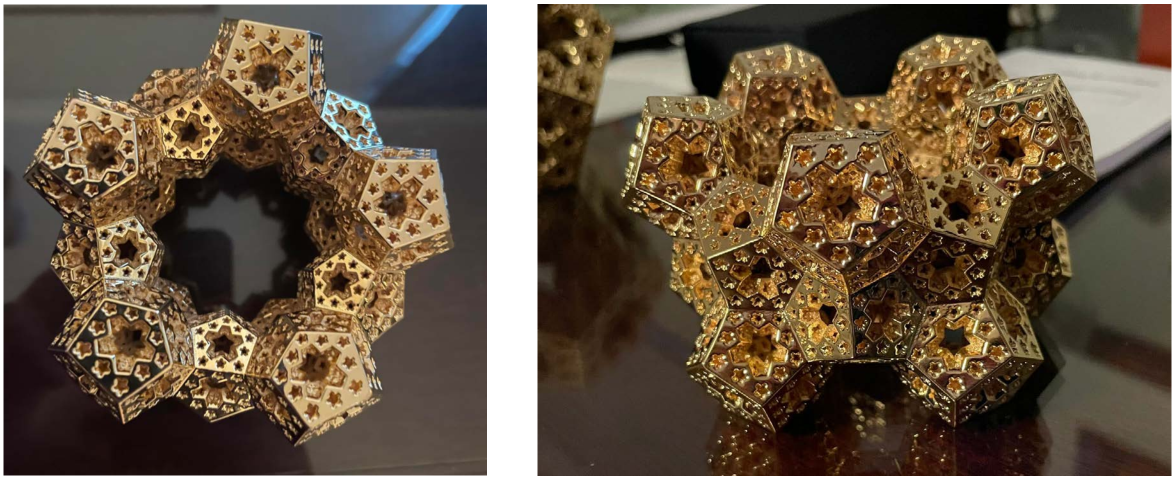

(a) (b)

Figure 9: *A torus-shaped conglomerate of four horizontal rings of ten fractal dodecahedrons each, taken from the fractal 120-cell.*

loop around the "trunk" of this tree, much like rings orbiting a planet. A 3D print of a particularly interesting collection of them is illustrated in Figure 9. All 3D prints are used as ornaments and other than the tree all are printed in brass plated with yellow gold, rose gold, or rhodium. In some cases, smaller versions may be worn as pendants. Work is underway to turn the tree-fractal into a decorative lamp.

Conclusions and Future Work

In this work, I have designed three variations of a fractal generalizing the Menger-slice, using pentagons and pentagrams rather than hexagons and hexagrams. I then generalized them to fractals based on the dodecahedron in 3D and the 120-cell in 4D, creating mathematical artwork that may be 3D printed. All three of my proposed generalizations are imperfect and other, better generalizations may still be out there, waiting to be discovered. This is my hope, and a project for another day.

References

[1] "Schlegel diagram." https://en.wikipedia.org/wiki/Schlegel_diagram.

[2] "Slice of Menger." https://flickr.com/photos/sbprzd/1432723128/.

[3] R. Hocking. "Three-Dimensional Diagonal Cross-Sections of Four-Dimensional Menger Sponges." *Proceedings of Bridges 2023: Mathematics, Art, Music, Architecture, Culture*. J. Holdener, E. Torrence, C. Fong, and K. Seaton, Eds. Phoenix, Arizona: Tessellations Publishing, 2023. pp. 291–298. http://archive.bridgesmathart.org/2023/bridges2023-291.html.

[4] M. McClure. "Directed-graph iterated function systems." *Mathematica in Education and Research*, vol. 9, no. 2, 2000, pp. 15–26.

[5] K. Menger. "Allgemeine Räume und Cartesische Räume. I." *Proc. Akad. Wet. Amsterdam*, vol. 29, 1926, pp. 476–482.

[6] H. Segerman and S. Schleimer. "Puzzling the 120-cell." *Notices of the AMS*, vol. 62, no. 11, 2015, pp. 1309–1316.

[7] J. Stillwell. "The Story of the 120-Cell, Volume 48, Number 1." 2000. https://api.semanticscholar.org/CorpusID:15502727.